Journal of ELECTRONIC MATERIALS, Vol. 39, No. 7, 2010
DOI: 10.1007/s11664-010-1191-7

Growth of HgTe Quantum Wells for IR to THz Detectors

S. DVORETSKY,[1,3] N. MIKHAILOV,[1] YU. SIDOROV,[1] V. SHVETS,[1] S. DANILOV,[2] B. WITTMAN,[2] and S. GANICHEV[2]

1.—A.V. Rzhanov Institute of Semiconductor Physics of SB RAS, Novosibirsk, Russia. 2.—Terahertz Center, University of Regensburg, 93040 Regensburg, Germany. 3.—e-mail: dvor@isp.nsc.ru

We zone-engineered HgCdTe/HgTe/HgCdTe quantum wells (QWs) using the molecular-beam epitaxy (MBE) method with *in situ* high-precision ellipsometric control of composition and thickness. The variations of ellipsometric parameters in the ψ–Δ plane were represented by smooth broken curves during HgTe QW growth with abrupt composition changes. The form of the spiral fragments and their extensions from fracture to fracture revealed the growing layer composition and its thickness. Single and multiple (up to 30) $Cd_xHg_{1-x}Te/HgTe/Cd_xHg_{1-x}Te$ QWs with abrupt changes of composition were grown reproducibly on (013) GaAs substrates. HgTe thickness was in the range of 16 nm to 22 nm, with the central portion of $Cd_xHg_{1-x}Te$ spacers doped by In to a concentration of 10^{14} cm^{-3} to 10^{17} cm^{-3}. Based on this research, high-quality (013)-grown HgTe QW structures can be used for all-electric detection of radiation ellipticity in a wide spectral range, from far-infrared (terahertz radiation) to mid-infrared wavelengths. Detection was demonstrated for various low-power continuous-wave (CW) lasers and high-power THz pulsed laser systems.

Key words: Growth, HgTe, HgCdTe, quantum wells (QWs), ellipsometric parameters, MBE, far-infrared, mid-infrared, detector

INTRODUCTION

Because of its unique physical properties, mercury cadmium telluride (MCT) ternary solid solution is the leading material for photonic infrared (IR) detectors operated over wide ranges of infrared wavelength and temperature.[1] An important problem in the development and production of large-format IR focal-plane array (FPA) is control of compositional uniformity (cutoff wavelength λ_c) throughout the thickness and over large areas, especially for long-wavelength infrared (LWIR) and THz ranges.

Nanostructures such as HgTe/CdTe superlattices (SLs), which have better wavelength cutoff uniformity than alloys, are an alternative material for IR detection.[2] However, the first experimental growth did not result in a high-quality HgTe/CdTe SL.[3]

(Received October 19, 2009; accepted March 10, 2010; published online April 14, 2010)

Recent technological advances in MBE have made it possible to grow a variety of HgTe/CdTe nanostructures suitable for fundamental investigations and device development. In particular, HgTe QW structures hold promise for fundamental studies of new physical phenomena[4,5] and as material for use in the rapidly developing field of spintronics.[6] In Ref. 7, $Cd_{0.65}Hg_{0.35}Te/Cd_{0.36}Hg_{0.64}Te$ (350 nm/250 nm thick) microcavity structures grown by MBE were used to fabricate 3-μm to 3.5-μm IR photoemitters. In Ref. 8, the authors demonstrated the growth of a doped HgTe/HgCdTe SL by MBE, which was then used for fabrication of very long-wavelength infrared (VLWIR) photodetectors (cutoff wavelength over 20 μm). The same group in Ref. 9 published results for high-quality MBE-grown HgTe/CdTe SLs on CdTe/Si with *in situ* high-energy electron diffraction and spectroscopic ellipsometry control of growth rate of only HgTe layers, but not of CdTe layers. From the theoretical analysis in Ref. 10, it is clear that HgTe/CdTe SLs are a very attractive

material for detectors operated in the LWIR and terahertz wavelength ranges. Improved control of wavelength cutoff must be achieved during the growth of inverted-band HgTe/CdTe SLs. However, normal-band HgTe/CdTe SLs are more promising for VLWIR detector applications.

Recently, a system for room-temperature electric detection of the polarization state of laser beams at terahertz frequencies by photogalvanic effects[11] was realized using low-symmetry GaAs and SiGe QWs.[12] The most attractive material for this type of detector is high-quality low-symmetry HgTe QWs, which is preferred over GaAs and SiGe because of its unique properties. In single HgTe QWs, large photogalvanic effects involving polarized laser beams from LWIR to THz ranges were found.[13] Terahertz conductivity in the Hall bar was observed in HgTe QWs under laser excitation with Ge active medium between 1.7 THz and 2.5 THz (corresponding to wavelengths of 120 μm to 180 μm).[14]

Single-wave ellipsometry was very effective for controlling MBE growth of HgCdTe alloys with designed composition profiles throughout the thickness for different IR detector applications.[15] Theoretical ellipsometric parameter trajectories were calculated for an MBE-grown HgTe/CdTe SL[16] and confirmed experimentally for HgCdTe potential barriers, wells, and periodical structures 100 nm in thickness.[17] The growth rate in these experiments reached 3.5 μm/h. The accuracy of MCT composition and thickness determination were $\Delta x \approx \pm 0.002$ mol fraction and $\Delta d \approx 1$ monolayer.

The technological problems associated with growing high-quality HgTe QWs and other HgCdTe-based nanostructures are well known. It is critical to develop a method for zone-engineering of high-quality single and multiple HgTe QWs with *in situ* compositional and thickness control for radiation detector applications.

We present the results of reproducible growth of single and multiple (up to 30) HgTe QWs with precise *in situ* single-wavelength ellipsometry control. We observed a large photogalvanic effect in single HgTe QWs in LWIR and THz spectral ranges compared with GaAs, Te, and multiple GaAs/GaAl/As QWs (20 QWs) and SiGe QWs structures. Multiple HgTe QWs showed a 25-fold increase in sensitivity compared with single QWs.

GROWTH OF HgTe QWs

Single and multiple HgTe-based QW structures are shown schematically in Fig. 1. QW growth was carried out with MBE equipment of Ob-M type.[18] The buffer layers of ZnTe (0.3 μm) and sequentially CdTe (5 μm to 7 μm) were grown on an atomically clean surface of (013) GaAs substrate prepared by chemical etching and thermal annealing in As flux in an ultrahigh-vacuum chamber.[19] Then 16 nm to 22 nm HgTe QWs with 24 nm $Hg_{1-x}Cd_xTe$ ($x \approx 0.7$) spacers were grown on the CdTe/ZnTe/GaAs at a

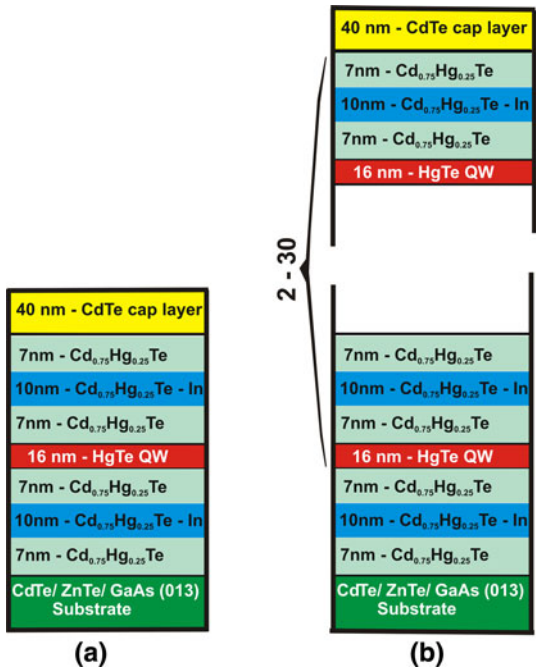

Fig. 1. Scheme of HgTe-based quantum wells: (a) single HgTe QW, and (b) multiple (2 to 30) HgTe QWs.

temperature between 180°C and 190°C. The central part (10 nm) of spacer was doped *in situ* to a carrier concentration of approximately 10^{15} cm^{-3} using a conventional indium source.[20] The growth rate was 0.15 μm/h. The MCT composition during the growth was varied by a cadmium flux. An ultrafast single-wavelength ($\lambda = 0.6328$) automatic ellipsometer (LEF-755; UFE) based on an original static scheme[21] was used for layer buffer thickness and MCT composition and thickness control.

On epitaxial growth of the layer on a substrate with different optical constants, damping oscillations of ellipsometric parameters ψ and Δ were observed. The number of oscillations depended on the absorption coefficient of the growing layer and decreased as the absorption coefficient increased. The oscillation amplitude was calculated as the difference of absorption coefficients of the substrate and the growing layer. One period of the oscillations corresponded to 100 nm of MCT layer growth. On growth of the multilayer structure with thickness lower than 100 nm, one should observe sectionally smooth curves corresponding to growth of MCT layers with constant composition. The length of the sectionally smooth curves corresponded to the growing layer thickness.

GROWTH OF HgTe SINGLE QWs

The evolution of the ellipsometric parameters Δ and ψ during the growth of a single HgTe-based QW (Fig. 1a) is shown in Fig. 2.[22] It is represented as a sectionally smooth curve in the ψ–Δ plane. Smooth sections correspond to growth of layers

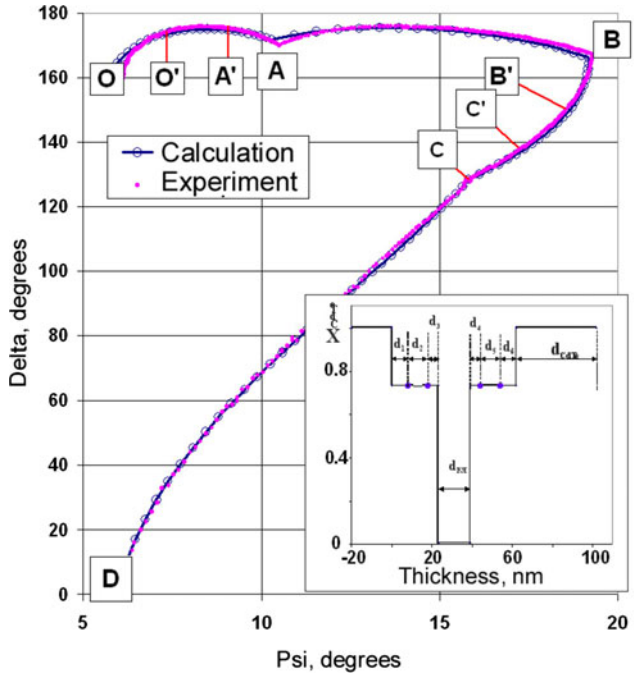

Fig. 2. Evolution of ellipsometric parameters Δ and ψ during the growth of HgTe-based QWs. Points at curve knees (O–C) correspond to the initial stage of growth of the following QW layer. *Dots*: experimental data; *solid line and circles* (interval 1 nm): calculated data. *Inset*: MCT composition variation with thickness.

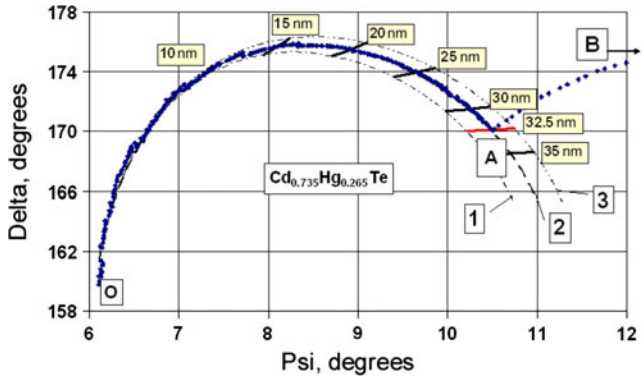

Fig. 3. Evolution of the ellipsometric parameters Δ and ψ during wide-gap layer growth on the CdTe surface. *Diamonds*: experimental data. Lines 1–3: MCT composition calculations (1, x_{CdTe} = 0.75; 2, x_{CdTe} = 0.735; 3, x_{CdTe} = 0.72). Lines transverse to OA correspond to equal thickness for different MCT compositions.

with constant MCT composition. Their length reflects the layer thickness. The initial point O corresponds to the ellipsometric parameters of the CdTe surface.

QW fabrication began at the first spacer layer ($x \approx 0.7$) growth (curve O–A) after the opening of the tellurium and cadmium source shutters. The doping of the central part of this layer was carried out by indium after opening (at O′) and closing (at A′) the indium source shutter. Then the growth of the wide-gap layer continued up to point A. In the inset to Fig. 2, the sectors O–O′, O′–A′, and A′–A correspond to parts of the spacer that are undoped with thickness d_1 and In-doped with thickness d_2, and the undoped wide-gap layer with thickness d_3, respectively. After closing the cadmium source shutter, a HgTe layer of thickness d_{QW} was grown, and the ellipsometric parameters Δ and ψ changed between points A–B as shown in the Δ–ψ plane in Fig. 2. The second spacer layer (curve B–C) grew in a manner analogous to the growth of the first spacer layer (curve O–A) after the opening of the cadmium source shutter. The thicknesses d_4, d_6, and d_5 correspond to the undoped, In-doped, and undoped parts of the second spacer layer. The grown single QW structure was covered by a CdTe cap layer of thickness $d_{CdTe} \approx 40$ nm.

The dots on the curve in Fig. 2 represent experimental data measured at 1-s intervals. The circles correspond to calculated values of the ellipsometric parameters at 1-nm thickness intervals. The calculations were carried out using a one-layer model.[23] The calibration curve and optical constants for calculation were used for different MCT compositions in Refs. 24 and 25. It was necessary to obtain accurate optical constants for the substrate and growing layers at incident light wavelength and growth temperature in order to improve the match between the experimental data and calculated values.

HgCdTe optical constants for different compositions were obtained from spectral measurements at room or lower temperature.[26,27] These data could not be used to calculate ellipsometric parameter variations during QW growth, which occurs at much higher temperature. Thus, we used the dependences of the optical constants, $n(x)$ and $k(x)$, on HgCdTe composition, which were measured at room temperature.[24] We then calculated the growth temperature using experimentally determined thermooptical coefficients. Generalizing all experiments, we obtained the following empirical formulas:

$$n(x) = 3.91 - 0.80x + 0.24x^2 + 0.184x^3, \quad (1)$$

$$k(x) = 1.318 - 1.829x + 0.987x^2 + 0.200x^3. \quad (2)$$

The experimental data agreed with calculations (Fig. 2) in this procedure.

The procedure for determining HgCdTe composition and layer thickness for a spacer layer grown on the CdTe surface is shown in more detail in Fig. 3. Point O corresponds to the ellipsometric parameters of the CdTe surface. The smooth variation of the ellipsometric parameters ψ and Δ in sector OA corresponds to spacer layer growth. The lines 1–3 represent the calculated values for the case of spacer growth layers with different HgCdTe compositions x = 0.75 (1), x = 0.735 (2), and x = 0.72 (3) with the following parameters: angle of incident light = 67.9 ± 0.05°, n_{CdTe} = 3.003, k_{CdTe} = 0.204, n_{HgTe} = 4.08, and k_{HgTe} = 1.16. These parameter values were determined using the measurement of

ellipsometric parameters during epitaxial growth of constant-composition HgCdTe alloys. The thickness of a growing spacer layer was determined using the length of the curve OA.

The thick lines transverse to the curve OA correspond to equal thickness for different HgCdTe compositions. The degree of mismatch between the experimental data, the calculated curves, and the position of the inflection point can be used to estimate the accuracy to which the HgCdTe composition and thickness of the growing layer can be measured. For the data in Fig. 2, the HgCdTe composition was determined to be $x = 0.735 \pm 0.002$ using the above procedure. The upper bound of thickness accuracy determination did not exceed 0.5 nm, or one monolayer. We carried out a similar analysis of other parts of the curve in Fig. 2. Thus, we determined the HgCdTe compositions and thicknesses of HgTe-based QWs. The accuracy of HgCdTe composition and thickness determination were $\Delta x \approx 0.002$ nm and 0.5 nm, respectively.

The MCT composition distribution throughout the thickness of HgCdTe-based QWs was measured by reflection spectra in the range of 1.5 eV to 6 eV with layer-by-layer chemical etching in 0.05% Br in HBr solution.[28] The positions of interference maxima were measured to better than 0.01 cm^{-1} using an Infralum FT-801 Fourier spectrometer. The accuracy of thickness determination was better than 0.1 nm. The results of measurements of MCT composition by *in situ* ellipsometry during growth and by reflection spectra with layer-by-layer chemical etching were in agreement.

Quantum Hall-effect investigations confirmed the high quality of the HgTe QWs.[4] The observed magnetoresistance behavior was consistent with that of a two-dimensional electron gas. Electron mobility at $T = 1.6$ K was 2.4×10^5 cm^2 V^{-1} s^{-1} to 3.5×10^5 cm^2 V^{-1} s^{-1} for an electron concentration of $N_s = 1.5 \times 10^{11}$ cm^{-2} to 3×10^{11} cm^{-2}, revealing the high quality of the QWs grown.

GROWTH OF MULTIPLE HgTe QWs

Multiple HgTe QWs (Fig. 1b) were grown as periodic HgTe QW structures with ellipsometric control of composition and layer thickness. The ellipsometric problem for a periodic layered structure was solved in an earlier paper.[29] The ellipsometric trajectory in the Ψ–Δ plane is represented by a curve with breaks at layer interfaces. After some layering cycles, the ellipsometric parameters vary periodically between two limiting points $P_1 = (\Psi_1, \Delta_1)$ and $P_2 = (\Psi_2, \Delta_2)$, corresponding to the structure with an upper layer and composition x_1 or x_2. Points $P_{1,2}$ and the ellipsometric trajectory depend on the layer compositions x_1 and x_2 and thicknesses d_1 and d_2 and may be calculated analytically and numerically for given parameters. The goal of *in situ* ellipsometric control is to maintain growth conditions supporting reproducible variation

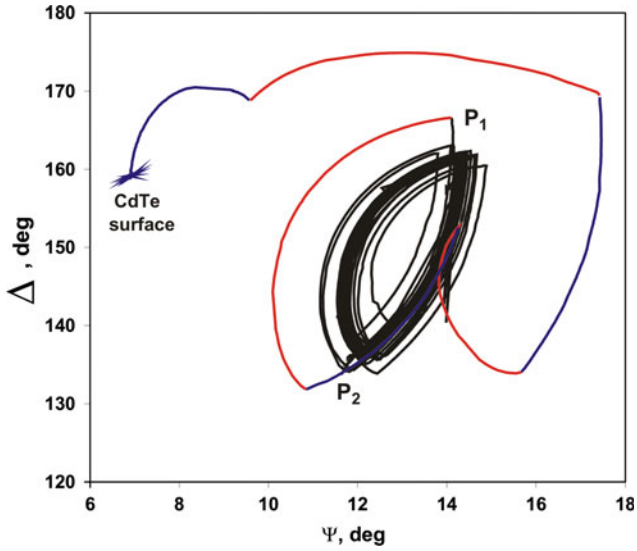

Fig. 4. Evolution of ellipsometric parameters Δ and ψ during the growth of multiple HgTe-based QWs. Points P_1 and P_2 correspond to periodicity of HgTe QW growth.

of Ψ and Δ between calculated points on the Ψ–Δ plane.

Figure 4 shows the experimental ellipsometric trajectory measured during the growth of multiple HgTe QWs. The curve breaks at each interface, and those after approximately ten alterations display a nearly reproducible variation between points P_1 and P_2. This proves the periodicity of the growing structure parameters of layer composition and thickness. The parameters may be determined by comparing the calculated and experimental trajectories.

Figure 5 shows one cycle of ellipsometric variations when growing a repeating pair of alternating structure layers. Squares correspond to experimental data, while solid curves represent various values of compositions (denoted by numbers near the curves). The calculations are based on the dependence of the optical constants of MCT on the composition, which was measured earlier, improved in experimental work,[24] and corrected for growth temperature[25] using the empirical formulas (1) and (2). The best fit for a spacer (wide-bandgap HgCdTe) layer is seen at $x = 0.76$. For a narrow-bandgap layer (HgTe QW), the best-fit curve with $x = 0.1$ yields only satisfactory agreement. However, appreciable deviations between experiment and calculation were observed for this layer at the initial growth stage. Comparing the experimental with the calculated data, we conclude that the composition was inhomogeneous at the initial stage and varied monotonically from $x \approx 0.3$ to $x \approx 0.1$. The layer thicknesses could be easily determined by analyzing the positions of the turning points $P_{1,2}$ at calculated curves, which were calibrated with thickness.

The procedure described above was used successively for all layers starting from the substrate.

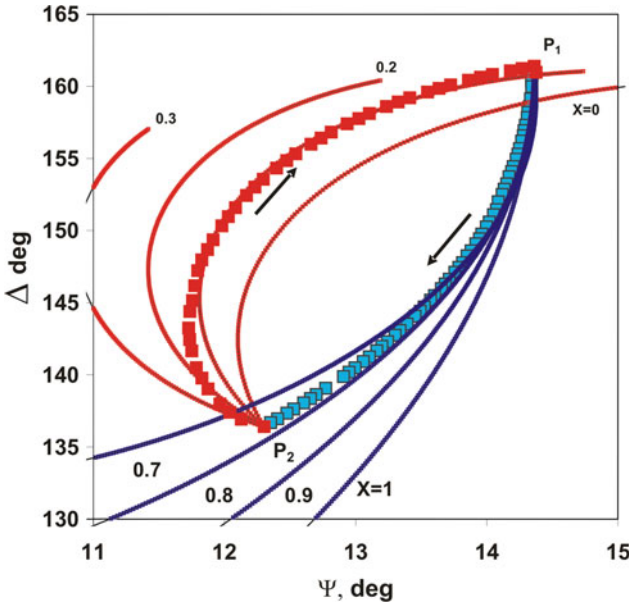

Fig. 5. Evolution of ellipsometric parameters Δ and ψ during one cycle. *Dots*: experimental data; *solid line*: calculated data. Arrows indicates the direction of ellipsometric parameters Δ and ψ during growth. P_1P_2: growth of HgCdTe spacer layer. P_2P_1: growth of HgTe layer.

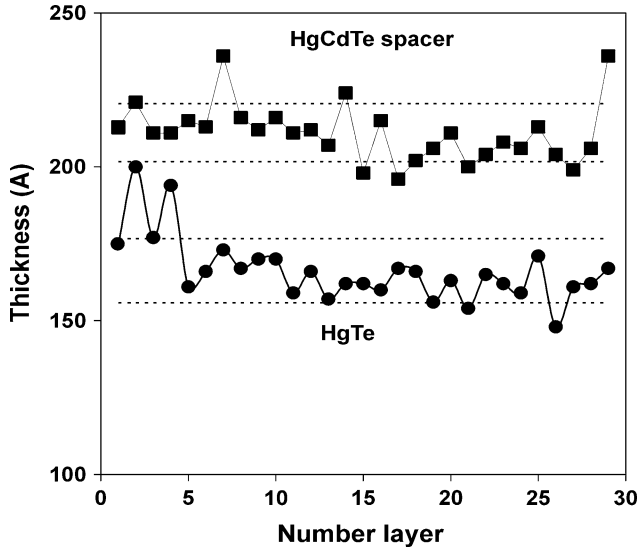

Fig. 6. HgTe and HgCdTe spacer layer in 30 HgTe QWs. *Solid lines*: average layer values; *dotted lines*: standard deviation. The average period of the structure is 37.7 nm (d_{HgCdTe} = 21.1 and d_{HgTe} = 16.6 nm).

For the $(j + 1)$-th layer, a multilayer structure should be considered as a complex substrate with reflection coefficients $R_{j(p,s)}$ for p- and s-polarizations of light. The calculation used the parameters determined in the preceding steps. We applied such an algorithm for periodic HgCdTe structure in Ref. 17. The possibility that the calculation of the $(j + 1)$-th layer parameters, being dependent on the measurements for all preceding layers, may suffer from error accumulation was unfortunately not realized, as may be shown by replacing the multilayer structure by homogeneous media with optical constants determined from ellipsometric measurements. Correctness of such replacements for semiconductor structures (including HgCdTe) was justified in Ref. 30. In this approach, the desired parameters of the current layer were calculated taking into account only the data measured during its growth. Therefore, all measurements performed for previous layers did not affect the result. In this case, calculations may be carried out for any chosen individual layer; for step-by-step algorithms, calculations start from the substrate.

Figure 6 shows the thicknesses of all layers of the multiple (30) HgTe QWs obtained from the experimental trajectory in Fig. 4 using the described method. The average period of the structure was 37.7 nm (d_{HgCdTe} = 21.1 nm and d_{HgTe} = 16.6 nm). There was some dispersion in thicknesses, even though the structure was periodic. The fabrication quality of the periodic structure could be improved by building in feedback control, implying automatic regulation (adjustment) of molecular sources based on ellipsometric measurements.

DETECTOR APPLICATIONS

High-quality HgTe QWs characterized by high electron mobilities, low effective masses, large g factors, and spin–orbit splitting of subbands in momentum space[31] possess great potential for detection of terahertz radiation[11,32,33] and in the rapidly developing field of spintronics.[22,34]

We demonstrated that HgTe QWs can be used for all-electric detection of radiation ellipticity in a wide spectral range, from far-infrared (terahertz radiation) to mid-infrared wavelengths. The most important property of the materials relevant for detection of radiation ellipticity is the magnitude of the circular photogalvanic effect (CPGE),[11,12,35] which gives access to the helicity of a radiation field. Such detection is seen in various low-power CW and high-power pulsed laser systems. In this study, a large spectral range was covered by low-pressure CW, pulsed and Q-switched CO_2 lasers, and high-power pulsed transverse excited atmospheric pressure (TEA) CO_2 lasers, which are used directly in the infrared range or as pump sources for THz molecular lasers. In addition, measurements were carried out with a free electron laser, chosen because of its tunability and short pulses.[13]

In the terahertz range, the magnitude of the circular photogalvanic effect (CPGE), which provides information on the radiation helicity in HgTe-based QWs, was substantially larger than that in GaAs QWs investigated previously.[11,35] This increased

photogalvanic signal, proportional to the number of stacked QWs, was observed in multiple QW samples with 30 HgTe QWs.

We also detected a significant CPGE response in the mid-infrared spectral range, attributable to the narrow band structure of HgTe-based QWs. The detector spectral behavior and subnanosecond time resolution had been demonstrated earlier.[13]

CONCLUSIONS

We have demonstrated growth of single and multiple HgTe quantum wells with precise control by single-wavelength ellipsometry, which allowed us to measure the composition and thickness of each layer during growth. The accuracy of measurement of composition and thickness were $\Delta x \approx 0.002$ nm and 0.5 nm, respectively. High-quality single and multiple (up to 30) HgTe QWs were grown on (013) CdTe/ZnTe/GaAs substrates. The HgTe thickness varied within the range of 16 nm to 22 nm. The composition of the $Hg_{1-x}Cd_xTe$ spacers was in the range $x \approx 0.7$ to 0.75. The central part of the spacers was doped by indium with varying concentrations.

The high quality of the HgTe QWs was confirmed by the presence of two-dimensional electron gas.

We demonstrated that the application of novel narrow-gap semiconductor low-dimensional materials based on high-quality (013)-grown HgTe quantum well structures allows all-electric detection of the polarization state of elliptically polarized radiation from the mid-infrared to the THz range. The sensitivity and linearity of the developed detection system were sufficient to characterize the polarization of laser radiation from low-power CW lasers to high-power laser pulses. The short relaxation time of free carriers in semiconductors at room temperature makes it possible to detect subnanosecond laser pulses.

ACKNOWLEDGEMENTS

The work was financially supported by Grant RBFR 09-02-00467-a, Grant No. 27/28 from the Russian Academy of Sciences, and the DFG.

REFERENCES

1. M.A. Kinch, *J. Electron. Mater.* 29, 809 (2000).
2. J.N. Schulman and T.C. McGill, *Appl. Phys. Lett.* 34, 663 (1979).
3. M.W. Goodwin, M.A. Kinch, and R.J. Koestner, *J. Vac. Sci. Technol.* A6, 2685 (1988).
4. E.B. Olshanetsky, S. Sassine, Z.D. Kvon, N.N. Mikhailov, S.A. Dvoretsky, J.C. Portal, and A.L. Aseev, *JETP Lett.* 84, 565 (2006).
5. Z.D. Kvon, E.B. Olshanetsky, D.A. Kozlov, N.N. Mikhailov, and S.A. Dvoretsky, *JETP Lett.* 87, 502 (2008).
6. M. König, S. Wiedmann, C. Brüne, A. Roth, H. Buhmann, L.W. Molenkamp, X.-L. Qi, and Sh.-Ch. Zhang, *Science* 318, 766 (2007).
7. J.P. Zanatta, F. Noel, P. Ballet, N. Hidadach, A. Million, G. Destefanis, E. Mottin, C. Kopp, E. Picard, and E. Hadji, *J. Electron. Mater.* 32, 602 (2003).
8. Y.D. Zhou, C.R. Becker, Y. Selament, Y. Chang, R. Ashokan, R.T. Boreiko, T. Aoki, D.J. Smith, A.L. Betz, and S. Sivananthan, *J. Electron. Mater.* 32, 608 (2003).
9. Y. Selament, Y.D. Zhou, J. Zhau, Y. Chang, C.R. Becker, R. Ashokan, C.H. Grein, and S. Sivananthan, *J. Electron. Mater.* 33, 503 (2004).
10. C.H. Grein, H. Jung, R. Sindh, and M.E. Flatte, *J. Electron. Mater.* 34, 905 (2005).
11. S.D. Ganichev and Prettl, *Intense Terahertz Excitation of Semiconductors* (Oxford: Oxford University Press, 2006).
12. S.D. Ganichev, J. Kiermaier, W. Weber, S.N. Danilov, D. Schuh, Ch. Gerl, W. Wegscheider, D. Bougeard, G. Abstreiter, and W. Prettl, *Appl. Phys. Lett.* 91, 091101 (2007).
13. S.N. Danilov, B. Wittmann, P. Olbrich, W. Eder, W. Prettl, L.E. Golub, E.V. Beregulin, Z.D. Kvon, N.N. Mikhailov, S.A. Dvoretsky, V.A. Shalygin, N.Q. Vinh, A.F.G. van der Meer, B. Murdin, and S.D. Ganichev, *J. Appl. Phys.* 105, 013106 (2009).
14. C. Stellmach, R. Bonk, Yu.B. Vasilyev, A. Hirsch, G. Hein, C.R. Becker, and G. Nachtwei, *Phys. Stat. Sol. (c)* 3, 2510 (2006).
15. V.S. Varavin, V.V. Vasiliev, S.A. Dvoretsky, N.N. Mikhailov, V.N. Ovsyuk, Yu.G. Sidorov, M.V. Suslyyakov, A.O. Yakushev, and A.L. Aseev, *Opto-Electron. Rev.* 11, 99 (2003).
16. A.V. Rzhanov, K.K. Svitashev, A.A. Mardezhov, and V.A. Shvets, *Doklady Akademii Nauk* 297, 604 (1987).
17. N.N. Mikhailov, R.N. Smirnov, S.A. Dvoretsky, Yu.G. Sidorov, V.A. Shvets, E.V. Spesivtsev, and S.V. Rykhlitski, *Int. J. Nanotechnol.* 3, 120 (2006).
18. Yu.G. Sidorov, S.A. Dvoretski, N.N. Mikhailov, M.V. Yakushev, V.S. Varavin, and A.P. Antsiferov, *J. Opt. Tech.* 67, 31 (2000).
19. M. Yakushev, A. Babenko, D. Ikusov, V. Kartashov, N. Mikhailov, I. Sabinina, Yu. Sidorov, and V. Vasiliev, *Proc. SPIE, 5957, 5957 OG* (2005).
20. V.S. Varavin, S.A. Dvoretskiĭ, D.G. Ikusov, N.N. Mikhailov, Yu.G. Sidorov, G.Yu. Sidorov, and M.V. Yakushev, *Semiconductors* 42, 648 (2008).
21. E.V. Spesivtsev and S.V. Rykhlitski. *Useful model "Ellipsometer". Licence No 16314. Bulletin "Useful Models. Industrial Samples*", 35 (20. 12. 2000) (In Russian).
22. S.A. Dvoretsky, D.G. Ikusov, D.Kh. Kvon, N.N. Mikhailov, N. Dai, R.N. Smirnov, Yu.G. Sidorov, and V.A. Shvets, *Optoelectron. Instrum. Data Process.* 43, 375 (2007).
23. V.A. Svets, S.V. Rykhlitski, E.V. Spesivtsev, N.A. Aulchenko, N.N. Mikhailov, S.A. Dvoretsky, Yu.G. Sidorov, and R.N. Smirnov, *Thin Solid Films* 455–456, 688 (2004).
24. K.K. Svitashev, S.A. Dvoretsky, Yu.G. Sidorov, and V.A. Shvets, *Cryst. Res. Technol.* 29, 931 (1994).
25. V.A. Shvets, N.N. Mikhailov, M.V. Yakushev, and E.V. Spesivtsev, *Proc. SPIE* 4900, 46 (2002).
26. H. Arwin and D.E. Aspnes, *J. Vac. Sci. Technol.* A2, 1316 (1984).
27. L. Vina, C. Umbach, M. Cardona, and L. Vodopjanov, *Phys. Rev. B* 29, 6752 (1984).
28. S.A. Dvoretsky, D.G. Ikusov, Z.D. Kvon, N.N. Mikhailov, V.G. Remesnik, R.N. Smirnov, Yu.G. Sidorov, and V.A. Shvets, *Semicond. Phys. Quantum Electr. Optoelectron.* 10, 47 (2007).
29. A.V. Rzhanov, K.K. Svitashev, A.A. Mardezhov, and V.A. Shvets, *Doklady Akademii Nauk* 298, 862 (1988).
30. V.A.Shvets, *Optika i spectroskopiya*, 107, 844 (2009) (in Russian). *Opt. Spectrosc.* (English in press).
31. Z.D. Kvon, S.N. Danilov, N.N. Mikhailov, S.A. Dvoretsky, and S.D. Ganichev, *Physica E* 40, 1885 (2008).
32. K. Sakai, *Terahertz Optoelectronics* (Berlin: Springer, 2005).
33. D.L. Woolard, J.O. Jensen, and R.J. Hwu, eds., *Terahertz Science and Technology for Military and Security Applications* (Singapore: World Scientific, 2007).
34. M.I. Dyakonov, ed., *Spin Physics in Semiconductors* (in the Springer series in solid state sciences, ed. M. Cardona, P. Fulde, K. von Klitzing, R. Merlin, H.-J. Queisser, and H. Störmer) (Berlin: Springer, 2008).
35. S.D. Ganichev, W. Weber, J. Kiermaier, S.N. Danilov, D. Schuh, W. Wegscheider, Ch. Gerl, D. Bougeard, G. Abstreiter, and W. Prettl, *J. Appl. Phys.* 103, 114504 (2008).